Reac Kinet Mech Cat (2014) 113:615–628
DOI 10.1007/s11144-014-0749-4

Induced self-cleaning properties towards Reactive Red 198 of the cement materials loaded with co-modified TiO_2/N,C photocatalysts

Magdalena Janus · Kamila Bubacz · Justyna Zatorska · Ewelina Kusiak-Nejman · Adam Czyżewski · Jacek Przepiórski · Antoni W. Morawski

Received: 20 March 2014 / Accepted: 29 June 2014 / Published online: 16 July 2014

Abstract The possibility of promoting the self-cleaning properties of the cement materials was verified by implementing the obtained nitrogen and carbon co-modified titania-based (TiO_2/N,C) photocatalysts into the cement plates. Additionally, unmodified TiO_2 (Grupa Azoty Zakłady Chemiczne POLICE S.A., Poland) and a commercial photocatalyst P25 (Evonik Industries AG, Germany) were used as reference materials. The impact of treatment temperature on the physicochemical properties of the obtained TiO_2/N,C additives was discussed. The photocatalytic activity of the prepared cement plates was evaluated trough the degradation of a model organic compound (Reactive Red 198) under UV–vis light. It was found that cement plates containing TiO_2/N,C photocatalyst calcined at 600 °C temperature exhibited the highest photocatalytic activity. The role of several factors such as crystallinity, phase composition and non-metals presence in the TiO_2/N,C additives on the self-clearing properties of the cement samples was also included in the discussion.

Keywords Self-cleaning · Cement · Photocatalysis · Titanium dioxide · TiO_2/N,C, azo-dye

M. Janus (✉) · K. Bubacz · J. Zatorska · E. Kusiak-Nejman · A. Czyżewski · J. Przepiórski · A. W. Morawski
Institute of Chemical and Environmental Engineering, West Pomerania University of Technology, Szczecin, ul. Pułaskiego 10, 70-322 Szczecin, Poland
e-mail: mjanus@zut.edu.pl

M. Janus
Department of Sanitary Engineering, West Pomerania University of Technology, al. Piastów 50, 70-310 Szczecin, Poland

Introduction

The photocatalytic properties of titanium dioxide (TiO_2) are commonly used for preparation of materials with self-cleaning properties, especially in order to enhance the esthetic durability of white cement materials. On the market, self-cleaning glasses or facade of buildings are present. The additive of nanocrystalline titania to photocatalytic building and construction materials is mainly due to the effectiveness under solar light irradiation, low production costs of titania powder, safety for environmental and compatibility with traditional building materials [1]. It is worth pointing out that the matter of nano-sized TiO_2 addition to construction materials remains controversial for many researchers whether TiO_2 particles enhanced the photocatalytic activity of building materials or they are only fine but non-reactive fillers.

Cements loaded with TiO_2 nanoparticles were used for photocatalytic degradation of gaseous and liquid environmental pollutions [2, 3]. Cárdenas et al. [4] reported the depollution activity of cement paste samples containing 0.0, 0.5, 1.0, 3.0 and 5.0 % of titanium dioxide nanoparticles towards degradation of nitrogen oxides NO_x. Additionally, the influence of type of titania phases was considered, proving that the highest NO_x degradation rate was observed for cement sample loaded with 5.0 % of anatase phase. Furthermore, the photocatalytic removal of organic compounds discharged to water, like organic dyes was also studied [5, 6]. For example, Folli et al. [7] proved that the cement sample loaded with TiO_2 exhibited self-cleaning properties during the photocatalytic tests conducted with the use of Rhodamine B dye. Moreover, modified cements can also reveal the antifouling properties. Graziani et al. [8] assessed the biocide effect of TiO_2 coatings applied on clay brick specimens under weak UV radiation. Results revealed that TiO_2 nanocoating was not able to fully prevent microalgal biofouling. However, the adhesion of these microorganisms was effectively prevented under optimal UV exposure conditions.

The self-cleaning abilities of building materials (loaded with TiO_2) frequently depend on physicochemical properties of the photocatalytic additive. It is generally claimed that structural parameters of TiO_2 such as crystallinity, particle size or surface area may impact the photocatalytic activity [9, 10]. Especially, a high rate of crystallinity and the presence of anatase phase have essential influence on the photocatalytic performance of the material [11]. The role of structural parameters of TiO_2-based photocatalysts on their photocatalytic activity towards degradation of the pollutant is not so unequivocally explicit. However, according to Baudys et al. [12], no direct correlation between well available commercial TiO_2 powders properties and photoactivity towards degradation of model dye Acid Orange 7 were found. It was discussed that even materials containing partly inactive rutile or exhibiting small specific surface area can display substantial photocatalytic properties.

In this study, the influence of the additive of titanium dioxide simultaneously modified with carbon and nitrogen on the enhancement of the photocatalytic activity of cement plates towards Reactive Red 198 degradation is discussed. It is well known that nitrogen or carbon TiO_2 doping is generally used for performing

photocatalytic reaction of titania nanopowders under visible light [13, 14]. Co-modification of TiO_2 with carbon and nitrogen enhanced the N,C-TiO_2 photoactivity utilizing visible light due to the synergetic effect of both carbon and nitrogen dopants in comparison to N-TiO_2 and C-TiO_2 photocatalysts [15–17]. Xu et al. [16] and Liu et al. [17] discussed the improvement of N,C–co-doped titania photocatalytic activity under visible light due to the synergetic effect of carbon and nitrogen dopants as well as the high surface roughness of titania films. Taking all of this aspects into account and also the fact that the N,C-TiO_2 photocatalyst will be used as an additive to cement powder, it was decided to apply co-doped titania powder as the material with the enhanced photocatalytic performance in comparison to N- or C-doped TiO_2.

Experimental

Materials

Titanium dioxide obtained by the sulfate technology from Grupa Azoty Zakłady Chemiczne POLICE S.A. (Poland) was used as a starting material. Commercial titania P25 (Evonik Industries AG, Germany) with the specific surface area of 55 m^2/g and the crystallite size of 21 nm for anatase (78.8 %) and 31 nm for rutile (21.2 %) was used as a reference material [18]. In many papers, it was reported that P25 nanopowder shows considerable inhomogeneity in the case of phase composition and crystallite sizes [18–21].

Synthetic ammonia (Messer Polska Sp. z o.o., Poland) and n-hexane solvent (POCH S.A., Poland) were used as nitrogen and carbon sources. High purity argon (99.999 %, Messer Polska Sp. z o.o., Poland) was used as an inert gas.

Portland cement CEM I 32.5R (Zakład Produkcyjny IZOLBET Sp. J., Poland) served as a base material used in the preparation of the cement and TiO_2/N,C composites (Cm-TiO_2/N,C).

An aqueous solution of monoazo dye Reactive Red 198–RR 198 (Boruta-Zachem S.A., Poland) with a concentration of 50 mg/dm^3 was used as a model organic contaminant.

TiO_2 and TiO_2/N,C photocatalysts preparation

20 g of starting TiO_2 was put in a quartz crucible and placed inside the 150 cm long quartz tube, which was an integral part of the horizontal furnace (Nabertherm GmbH, Germany). The argon gas, with the flow of 200 cm^3/min, was passed through a quartz tube for 0.5 h to remove the air from the interior. Afterwards, the gas flow was reduced to 100 cm^3/min and the TiO_2 sample was heat-treated with a heating rate of 5 °C/min. The furnace was programmed to reach one of the desired treatment temperature (100 °C or 300 °C or 600 °C), and maintain the final temperature for additional 1.5 h. After that time, the photocatalyst samples were cooled down under constant argon gas flow (100 cm^3/min).

The preparation procedure of co-modified TiO_2/N,C samples was similar to the one presented above. However, after reaching the desired temperature (100 °C or 300 °C or 600 °C), the inert gas was replaced by gaseous ammonia, passed (200 cm^3/min) through the Dreschel bottle containing 50 cm^3 of n-hexane. The ammonia flow was maintained for the duration of 1 h.

Cement–TiO_2 and cement–TiO_2/N,C mixtures preparation

Appropriate amounts of Portland cement and 1 wt% or 10 wt% of co-modified TiO_2/N,C photocatalyst were pounded in a porcelain mortar, to obtain homogenous cement and unmodified TiO_2 (Cm-TiO_2) or cement and co-modified TiO_2/N,C (Cm-TiO_2/N,C) powders. Prior to further use, all of the prepared mixtures were dried at 105 °C for 24 h and subsequently stored in a desiccator.

Forming of cement plates containing TiO_2 or TiO_2/N,C photocatalyst

10 g of Cm-TiO_2 (or Cm-TiO_2/N,C) powder was mixed with 5 cm^3 of water. The obtained slurry was purred into silicone mould (2 cm × 2 cm × 0.6 cm) and set aside for solidification of the material. In the case of cement-P25 (Cm-P25) composites, the addition of the commercial photocatalyst led to significant increase of cement paste density. Due to this fact, it was necessary to increase the amount of water added to the material (to 8 cm^3), and thus to inhibit the rapid setting of the cement component.

Photocatalytic activity tests

The photocatalytic activity of the prepared cement plates was determined during decomposition of RR 198 under UV–vis irradiation tests. To this end, the single cement plate was dipped into 8 cm^3 of RR 198 aqueous solution for 1 h and then dried for 24 h at 105 °C. The irradiation of the cement plates was conducted for 8 h, using six UV–vis lamps (Philips Cleo, 20 W each) with the radiation intensity of 109.7 W/m^2 and 115.2 W/m^2 for UV and vis, respectively. The recorded emission spectrum of the UV–vis lamps is presented in Fig. 1. The distance between the cement plate and the UV–vis lamps (ca. 24 cm) was kept constant during all conducted irradiation tests.

Material characterization

The TiO_2/N,C photocatalysts and cement plates were characterized by UV–Vis/DR using V-630 spectrophotometer (Jasco Corporation, Japan) equipped with an integrating sphere accessory for diffuse reflectance spectra ($BaSO_4$ was used as a reference material). FTIR/DR spectra of tested photocatalysts were recorded using FT/IR 4200 spectrometer (Jasco Corporation, Japan) equipped with DR accessory of Harrick Scientific Products, Inc. (USA). X-ray diffraction patterns were obtained by applying X'Pert PRO diffractometer (PANalytical B.V., USA) with Cu K_α radiation ($\lambda = 1.54056$ Å). The BET specific surface areas were calculation on the bases of

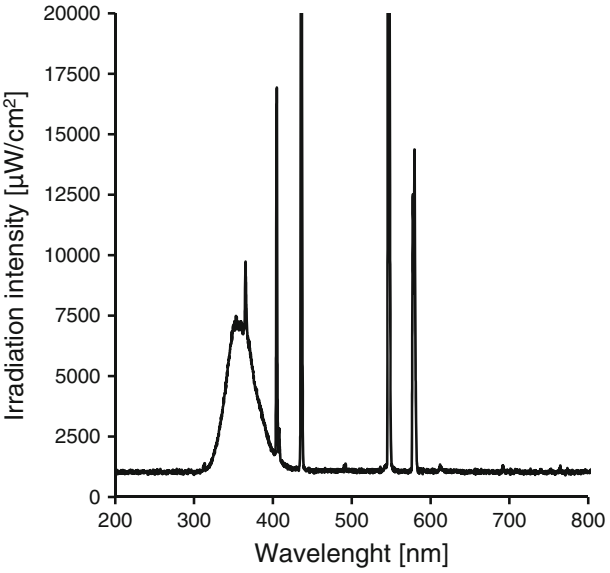

Fig. 1 The emission spectrum of the UV–vis lamps

the N_2 adsorption measurements conducted at 77 K using Quadrasorb SI analyzer (Quantachrome Instruments, USA). The carbon content measurements were conducted using Multi N/C 2000 analyzer (Analytik Jena AG, Germany) with the option for solid samples. The nitrogen content in TiO_2/N,C photocatalysts samples was estimated using ONH 836 analyzer (Leco Corporation, USA). The radiation intensity of UV–vis irradiation source was measured using radiation intensity meter LB 901 (Lab-El Sp. J., Poland) equipped with CM3 and PD204AB Cos sensors.

Results and discussion

Photocatalyst characteristics

The FTIR/DRS spectra of unmodified and co-modified photocatalysts, calcined at different temperatures are shown in Fig. 2a–c. First, the wide bands visible at the range of 3,300–3,695 cm^{-1} can be attributed to hydroxyl groups and water adsorbed on the photocatalysts surface [22]. The presence of water is also confirmed by the band located at 1,637 cm^{-1}, assigned to the molecular water-bending mode [23]. It is worth pointing out that, in the case of unmodified and co-modified samples (Fig. 2a and b), the increase of treatment temperature resulted in the decrease of bands intensity apparent in the wavelength range of 3,300–3,695 cm^{-1}. This mutual effect is most likely caused by the releasing of water molecules present on the surface of the materials. The additional band at 1,415 cm^{-1} visible on the spectrums of co-modified photocatalysts (Fig. 2b) can be assigned to nitrogen groups [23] and

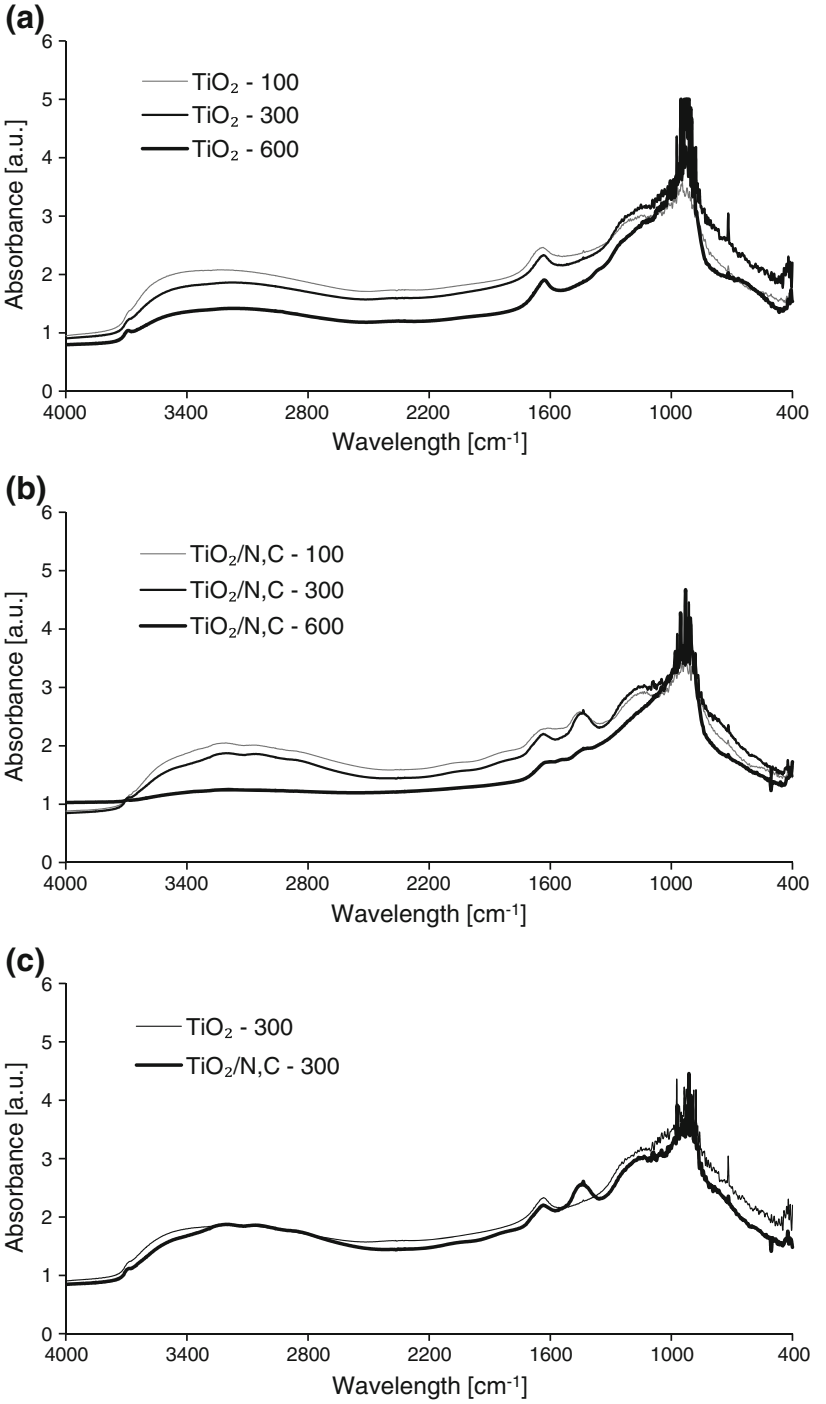

Fig. 2 The FT-IR/DRS spectra of the unmodified and the N, C co-modified photocatalysts

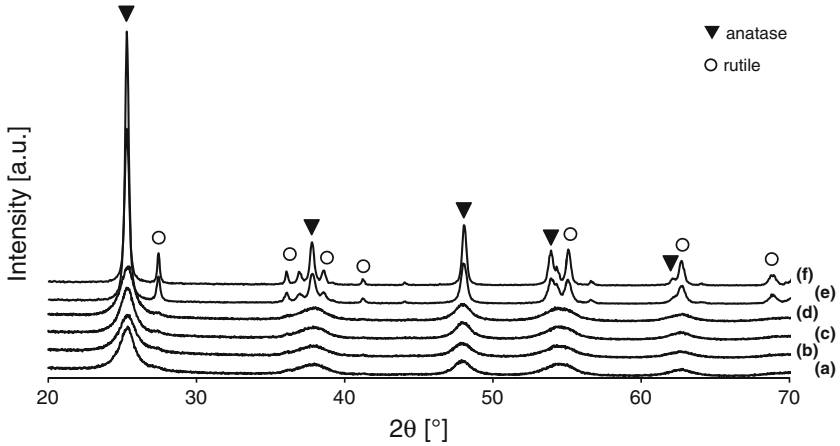

Fig. 3 The XRD patterns of: **a** TiO_2-100, **b** TiO_2/N,C-100, **c** TiO_2-300, **d** TiO_2/N,C-300, **e** TiO_2-600, and **f** TiO_2/N,C-600 photocatalysts

carbon species [24]. Furthermore, it should be noted that the spectrums comparison of the TiO_2-300 and TiO_2/N,C-300 photocatalytic samples, heat-treated at the same temperature (Fig. 2c), allows to state that the performed N,C modification did not influence the content of the hydroxyl groups on the surface of the TiO_2/N,C photocatalyst.

The phase characteristics of starting TiO_2 and co-doped TiO_2/N,C calcined at different temperature was investigated by XRD analysis. As shown in Fig. 3, the anatase phase was a predominant structure in all samples, treated at 100 °C and 300 °C. The peak positioning, corresponding to the TiO_2 anatase phase were in accordance with the literature data [25]. In the case of the samples calcined at 600 °C, distinct peaks related to the rutile phase were also visible on the X-ray diffraction spectrums.

The effect of physicochemical properties and photocatalyst loading on photocatalytic activity of cement plates containing TiO_2 or TiO_2/N,C photocatalyst

Cement plates containing TiO_2 or TiO_2/N,C photocatalyst were used in RR 198 photocatalytic decomposition test. The dye removal rates on the respective cement samples, containing 1 wt% or 10 wt%, measured after subsequent hours of the UV–vis irradiation, are shown in Figs. 4 and 5, respectively.

In the case of the cement samples containing 1 wt% of the unmodified or co-modified TiO_2 photocatalysts, the maximum rate of removal varied in range from ca. 34–70 % (after 8 h of irradiation). The increase of photocatalyst content in the sample (up to 10 wt%) was reflected by the higher RR 198 degradation rate on cement plates. However, the removal of the dye was not so significant as expected. This observation concerned especially cement plates containing photocatalysts calcined at 100 °C and 300 °C (Figs. 4a, b, 5a, and b). It can be explained by the

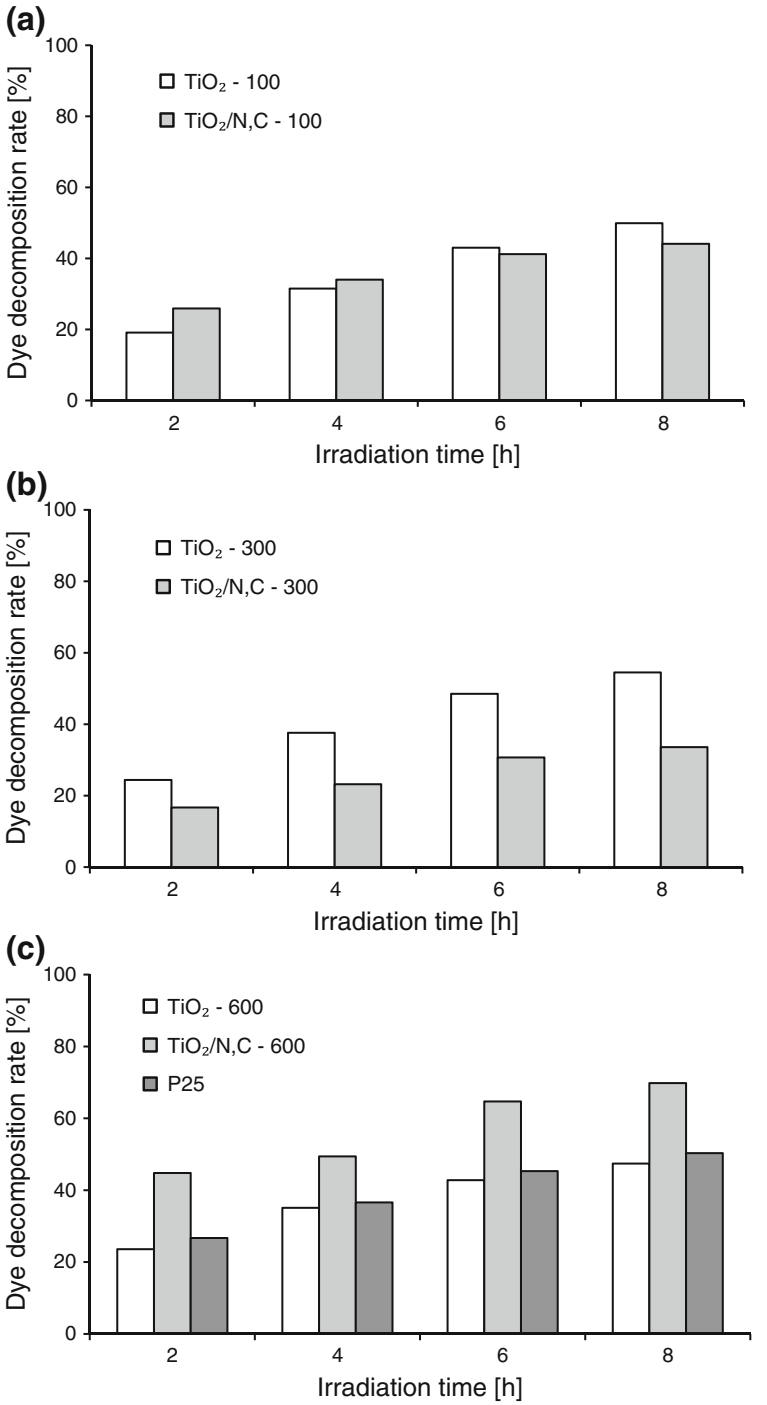
(a)
Dye decomposition rate [%]
100
80
60
40
20
0
TiO2 - 100
TiO2/N,C - 100
2
4
6
8
Irradiation time [h]
(b)
Dye decomposition rate [%]
100
80
60
40
20
0
TiO2 - 300
TiO2/N,C - 300
2
4
6
8
Irradiation time [h]
(c)
Dye decomposition rate [%]
100
80
60
40
20
0
TiO2 - 600
TiO2/N,C - 600
P25
2
4
6
8
Irradiation time [h]

◀**Fig. 4** The effectiveness of RR 198 photocatalytic degradation under UV irradiation on cement plates containing 1 wt% unmodified and modified photocatalysts calcined at different temperatures

increase of electron–hole recombination rate leading to a partial deactivation of photocatalyst active sites [26]. This effect is directly connected with insufficient quantity of species pre-adsorbed on photocatalyst surface, which act as carrier traps (e.g. oxygen) in comparison to amount of generated charge carriers [27]. However, it is worth pointing out that the best photocatalytic activity was achieved during photocatalytic process, in which the cement plate containing 10 wt% of TiO_2/N,C-600 photocatalyst was applied. In the case of this material, after 8 h of irradiation, the dye removal rate reached approximately 100 %. Furthermore, it should be noted that this material (Cm-TiO_2/N,C-600) displayed higher self-cleaning abilities than the comparative cement sample, containing 1 wt% or 10 wt% of commercial photocatalysts P25 or unmodified TiO_2 treated at 600 °C (Figs. 4c and 5c).

The observed tendencies of cement plate discoloration were connected with physicochemical properties of the studied photocatalysts added to the cement paste. The crystallinity of the photocatalytic additives, as well as its non-metal modification had a significant impact on the RR 198 degradation rate on cement plates. It ought to be stated that the TiO_2 additives heated treat at 100 °C or 300 °C temperatures had no significant influence on the anatase crystallite size values (Table 1). However, the increase of treatment temperature up to 600 °C resulted in considerable increase of the crystallite size of the anatase phase, considered as the most desired structure in terms of efficiency of the photocatalytic processes [28]. The presence of anatase phase is connected with the facility of efficient electron transport and the avoidance of the fast charge recombination [29]. Consequently, the presence of anatase crystalline structure influences the higher production of $^{\bullet}OH$ radicals (the main oxidative species in photocatalysis), in comparison to rutile [30, 31]. Furthermore, despite fact that the applying higher treatment temperature (600 °C) caused partial phase transformation of anatase to rutile, the remaining amount of the anatase structure (Table 1) was sufficient to maintain the photocatalytic properties of the material.

In reference to the non-metals appearance in TiO_2 lattice, the literature data generally stated that present as such species influence the photocatalytic response of the semiconductors [32]. In the case of the TiO_2 modification with nitrogen and carbon, the observed increase of the photocatalytic activity of the material is explained by the inhibition of the photoinduced electrons and holes recombination process [33, 34] and by the reduction of the energy required in the photocatalyst excitation [35]. Moreover, it is worth pointing out that the content of the dopants in TiO_2 lattice also impacts photocatalytic properties of TiO_2 [36]. For example, the high content of nitrogen in TiO_2 lattice influences the shifting of stable titania phase towards rutile [37]. In the case of our studies, the content of nitrogen in modified photocatalysts distinctly decreased with the treatment temperature, from 1.27 wt% to 0.22 wt% (for 100 °C and 600 °C, respectively). However, Dunnill et al. [38] confirmed that the even small quantities of nitrogen in the TiO_2 structure (0.15–0.70 at% according to XPS results) can lead to the enhancement of the photocatalytic

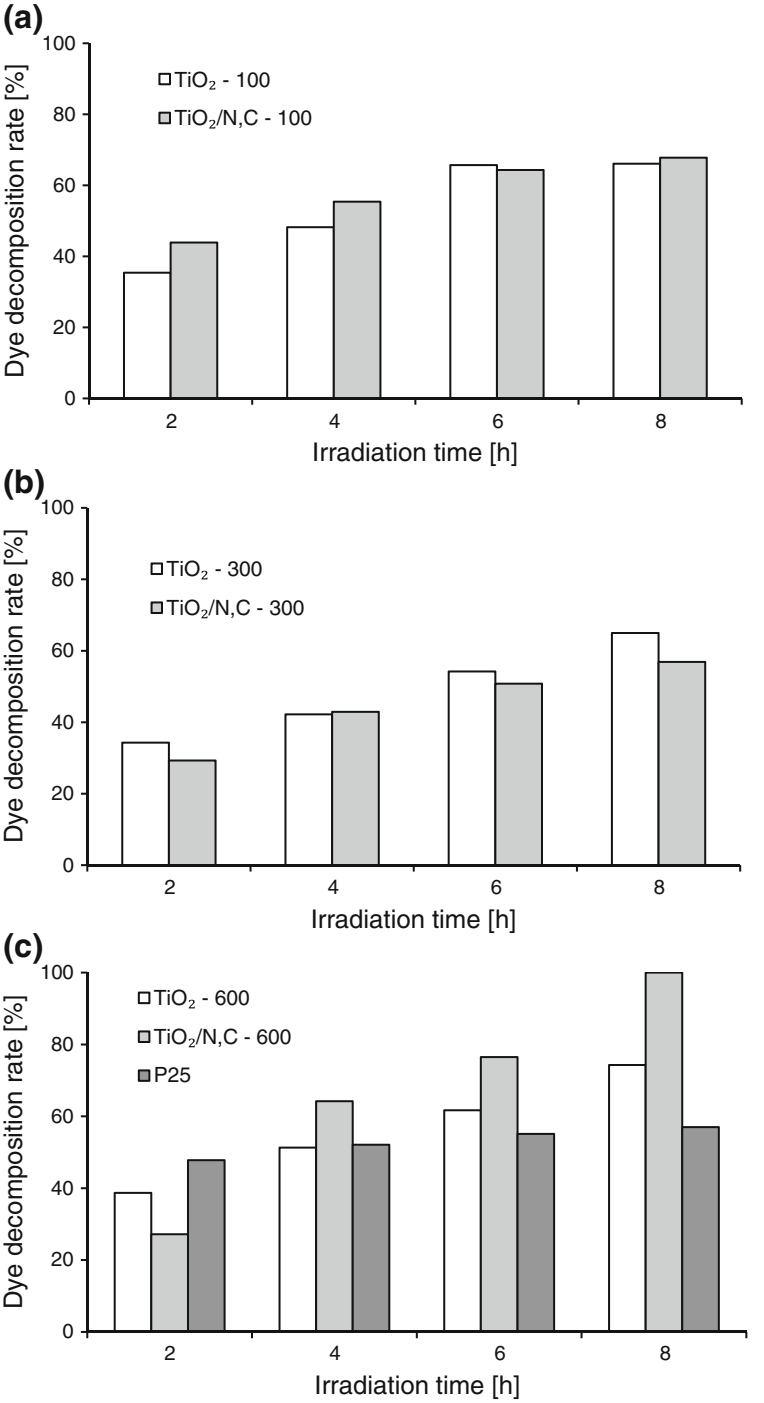
(a)
Dye decomposition rate [%]
100
80
60
40
20
0
TiO2 - 100
TiO2/N,C - 100
2
4
6
8
Irradiation time [h]
(b)
Dye decomposition rate [%]
100
80
60
40
20
0
TiO2 - 300
TiO2/N,C - 300
2
4
6
8
Irradiation time [h]
(c)
Dye decomposition rate [%]
100
80
60
40
20
0
TiO2 - 600
TiO2/N,C - 600
P25
2
4
6
8
Irradiation time [h]

◀**Fig. 5** The effectiveness of RR 198 photocatalytic degradation under UV irradiation on cement plates containing 10 wt% unmodified and modified photocatalysts calcined at different temperatures

Table 1 Physicochemical properties of the N,C co-modified and unmodified photocatalysts

Photocatalyst	S_{BET} (m^2/g)	Anatase crystallite size (nm)	Nitrogen content (wt%)	Carbon content (wt%)
TiO_2-100	249	7.6	–	–
TiO_2/N,C-100	219	6.7	1.27	0.12
TiO_2-300	241	7.8	–	–
TiO_2/N,C-300	206	7.7	0.97	0.05
TiO_2-600	58	29.0	–	–
TiO_2/N,C-600	24	50.0	0.22	0.14

properties of the TiO_2 films. Similar results were reported by Miyauchi et al. [39], confirming that the samples with the lowest content of nitrogen in TiO_2 (0.90 at%) revealed the highest photocatalytic activity. On the other hand, the photocatalytic response of the tested cement plates should be also related with the carbon content in N,C-TiO_2 photocatalysts. Wong et al. [40] discussed the enhancement of the photoactivity of the TiO_2–C film as the influence of carbon content and crystallinity of the carbon-modified TiO_2 materials. The best results were obtained for TiO_2-C film with an optimal carbon content. According to Palanivelu et al. [41] addition of C-impurity gives the semiconductor TiO_2 an excess of conducting electrons or an excess of conducting holes and the carbon doped titania contained less than 1 wt% of carbon. The influence of the carbon content in the photocatalysts on the photocatalytic activity of cement plates can be clearly observed, by comparing the TiO_2/N,C-100 and TiO_2/N,C-300 samples (Table 1). Moreover, taking into account the similar S_{BET} values of the discussed samples, the impact of this factor on the dye degradation cannot be clearly stated. The significantly higher carbon content in the TiO_2/N,C-100 photocatalyst might be the cause of the noticeably higher RR 198 removal rate on the cement plate (Cm-TiO_2/N,C-100). However, it should be stated that the excess of non-metal dopants in TiO_2 can result in a higher degree of structural defects of the co-modified photocatalysts, which can act as the centres of charge recombination [39]. This effect is reflected by the results of photocatalytic tests (Figs. 4 and 5), conducted for the unmodified and co-modified TiO_2 photocatalysts calcined at 100 °C and 300 °C. Furthermore, it should be noted that the tested cement plates loaded with TiO_2/N,C-600 photocatalyst (containing 0.22 wt% and 0.14 wt% of nitrogen and carbon, respectively), displayed the highest decomposition rate of the dye. Thus, it can be stated that the given nitrogen and carbon values were optional for achieving the best photocatalytic performance of the co-modified titania.

Conclusion

In this work, the influence of crystallinity, phase composition and non-metals content in the TiO_2/N,C additives to cement powder on the self-cleaning properties of the cement samples was studied. The enhancement of cementitious materials photoactivity is primarily related to the content of nitrogen, carbon in tested samples. Total discoloration of RR198 dye was observed on cement plates containing 10 wt% of TiO_2/N,C-600 photocatalyst, after 8 h of UV–vis light irradiation. The high photocatalytic activity of the latter cement material was related with the high rate of crystallinity and the presence of anatase phase in the co-modified TiO_2-based additive.

Acknowledgments Project was funded by the National Science Centre allocated on the basis of a decision number DEC-2011/01/D/ST5/03467.

References

1. Essawy AA, El Abd, Aleem S (2013) Physico-mechanical properties, potent adsorptive and photocatalytic efficacies of sulfate resisting cement blends containing micro silica and nano-TiO_2. Constr Build Mater 52:1–8
2. Chen J, Kou S-C, Poon C-S (2011) Photocatalytic cement-based materials: comparison of nitrogen oxides and toluene removal potentials and evaluation of self-cleaning performance. Build Environ 46:1827–1833
3. Lackhoff M, Prieto X, Nestle N, Dehn F, Niessner R (2003) Photocatalytic activity of semiconductor-modified cement–influence of semiconductor type and cement ageing. Appl Catal B Environ 43:205–216
4. Cárdenas C, Tobón JI, García C, Vila J (2012) Functionalized buildings materials: photocatalytic abatement of NO_x by cement pastes blended with TiO_2 nanoparticles. Constr Build Mater 36:820–825
5. Senff L, Tobaldi DM, Lemes-Rachadel P, Labrincha JA, Hotza D (2014) The influence of TiO_2 and ZnO powder mixtures on photocatalytic activity and rheological behavior of cement pastes. Constr Build Mater 65:191–200
6. Yousefi A, Allahverdi A, Hejazi P (2013) Effective dispersion of nano-TiO_2 powder for enhancement of photocatalytic properties in cement mixes. Constr Build Mater 41:224–230
7. Folli A, Pade C, Bæk Hansen T, De Marco T, Macphee DE (2012) TiO_2 photocatalysis in cementitious systems: insights into self-cleaning and depollution chemistry. Cem Concr Res 42:539–548
8. Graziani L, Quagliarini E, Osimani A, Aquilanti L, Clement F, Yéprémian C, Lariccia V, Amoroso S, D'Orazio M (2013) Evaluation of inhibitory effect of TiO_2 nanocoatings against microalgal growth on clay brick facades under weak UV exposure conditions. Build Environ 64:38–45
9. He F, Ma F, Li J, Li T, Li G (2014) Effect of calcination temperature on the structural properties and photocatalytic activities of solvothermal synthesized TiO_2 hollow nanoparticles. Ceram Int 40:6441–6446
10. Kim DS, Kwak S-Y (2007) The hydrothermal synthesis of mesoporous TiO_2 with high crystallinity, thermal stability, large surface area, and enhanced photocatalytic activity. Appl Catal A Gen 323:110–118
11. Trenczek-Zajac A, Radecka M, Jasinski M, Michalow KA, Rekas M, Kusior E, Zakrzewska K, Heel A, Graule T, Kowalski K (2009) Influence of Cr on structural and optical properties of TiO_2: Cr nanopowders prepared by flame spray synthesis. J Power Sources 194:104–111

12. Baudys M, Zlámal M, Krýsa J, Jirkovský J, Kluson P (2012) Notes on heterogeneous photocatalysis with the model azo dye acid orange 7 on TiO_2. React Kinet Mech Catal 106:297–311
13. Janus M, Tryba B, Kusiak E, Tsumura T, Toyoda M, Inagaki M, Morawski AW (2009) TiO_2 nanoparticles with high photocatalytic activity under visible light. Catal Lett 128:36–39
14. Kusiak-Nejman E, Janus M, Grzmil B, Morawski AW (2011) Methylene Blue decomposition under visible light irradiation in the presence of carbon- modified TiO_2 photocatalysts. J Photochem Photobiol A 226:68–72
15. Chen D, Jiang Z, Geng J, Wang Q, Yang D (2007) Carbon and nitrogen co-doped TiO_2 with enhanced visible-light activity. Ind Eng Chem Res 46:2741–2746
16. Xu QC, Wellia DV, Yan S, Liao DW, Lim TM, Tan TT (2011) Enhanced photocatalytic activity of C-N-codoped TiO_2 films prepared via an organic-free approach. J Hazard Mater 188:172–180
17. Liu G, Han C, Pelaez M, Zhu D, Liao S, Likodimos V, Kantos AG, Falaras P, Dionysoiu DD (2013) Enhanced visible light photocatalytic activity of N-C-co-doped TiO_2 films for the degradation of microcystin-LR. J Mol Catal A Chem 372:58–65
18. Porter JF, Li YG, Chan CK (1999) The effect of calcination on the microstructural characteristics and photoreactivity of Degussa P-25 TiO_2. J Mater Sci 34:1523–1531
19. Bakardjieva S, Šubrt J, Štengl V, Dianez MJ, Sayagues MJ (2005) Photoactivity of anataserutile TiO_2 nanocrystalline mixtures obtained by heat treatment of homogeneously precipitated anatase. Appl Catal B 58:193–202
20. Raj KJA, Viswanathan B (2009) Effect of surface area, pore volume and particle size of P25 titania on the transformation of anatase to rutile. Indian J Chem 48:1378–1382
21. Ohtani B, Prieto-Mahaney OO, Li D, Abe R (2010) What is Degussa (Evonik) P25 crystalline composition analysis, reconstruction from isolated pure particles and photocatalytic activity test. J Photochem Photobiol A 216:179–182
22. Wawrzyniak B, Morawski AW (2006) Solar-light-induced photocatalytic decomposition of two azo dyes on new TiO_2 photocatalyst containing nitrogen. Appl Catal B 62:150–158
23. Randorn S, Wongnawa P, Boonsin P (2004) Bleaching of methylene blue by hydrated titanium dioxide. Sci Asia 30:149–156
24. Lande M, Navgire M, Rathod S, Katkar S, Yelwande A, Arbad B (2012) An efficient green synthesis of quinoxaline derivatives using carbon-doped MoO_3-TiO_2 as a heterogeneous catalyst. J Ind Eng Chem 18:277–282
25. Ananpattarachai J, Kajitvichyanukul P, Seraphin S (2009) Visible light absorption ability and photocatalytic oxidation activity of various interstitial N-doped TiO_2 prepared from different nitrogen dopants. J Hazard Mater 168:253–261
26. Lucas SS, Ferreira VM, Barroso de Aguiar JL (2013) Incorporation of titanium dioxide nanoparticles in mortars. Influence of microstructure in the hardened state properties and photocatalytic activity. Cem Concr Res 43:112–120
27. Fox MA, Dulay MT (1993) Heterogeneous photocatalysis. Chem Rev 93:341–357
28. Xie M, Jing L, Zhou J, Lin J, Fu H (2009) Synthesis of nanocrystalline anatase TiO_2 by one-pot two-phase separated hydrolysis-solvothermal processes and its high activity for photocatalytic degradation of rhodamine B. J Hazard Mater 176:139–145
29. Xia B, Huang H, Xie Y (1999) Heat treatment on TiO_2 nanoparticles prepared by vapour-phase hydrolysis. Mat Sci Eng B Solid 57:150–154
30. Hirakawa T, Yawata K, Nosaka Y (2007) Photocatalytic reactivity for $^{\bullet}O^{2-}$ and $^{\bullet}OH$ radical formation in anatase and rutile TiO_2 suspension as the effect of H_2O_2 addition. Appl Catal A 325:105–111
31. Tryba B, Toyoda M, Morawski AW, Nonaka R, Inagaki M (2007) Photocatalytic activity and $^{\bullet}OH$ radical formation on TiO_2 in the relations to crystallinity. Appl Catal B 71:163–168
32. Giannakas AE, Seristatidou E, Deligiannakis Y, Konstantinou I (2013) Photocatalytic activity of N-doped and N–F co-doped TiO_2 and reduction of chromium (VI) in aqueous solution: an EPR study. Appl Catal B 132–133:460–468
33. Wang X, Lim TT (2010) Solvothermal synthesis of C-N co-doped TiO_2 and photocatalytic evaluation for bisphenol A degradation using a visible-light irradiated LED photoreactor. Appl Catal B 100:355–364
34. Linsebigler AL, Lu G, Yates JT (1995) Photocatalysis on TiO_2 surfaces: principles, mechanisms and selected results. Chem Rev 95:735–758
35. Yun HJ, Lee DM, Yu S, Yoon J, Park HJ, Yi J (2013) Effect of valence band energy on the photocatalytic performance of N-doped TiO_2 for the production of O_2 via the oxidation of water by visible light. J Mol Catal A 378:221–226

36. Mekprasart W, Khumtong T, Rattanarak J, Techitdheera W, Pecharapa W (2013) Effect of nitrogen doping on optical and photocatalytic properties of TiO_2 thin film prepared by spin coating process. Energy Procedia 34:746–750
37. Okato T, Sakano T, Obara M (2005) Suppression of photocatalytic efficiency in highly N doped anatase films. Phys Rev B 72:115–124
38. Dunnill CWH, Aiken ZA, Pratten J, Wilson M, Morgan DJ, Parkin IP (2009) Enhanced photocatalytic activity under visible light in N-doped TiO_2 thin films produced by APCVD preparations using t-butylamine as a nitrogen source and their potential for antibacterial films. J Photochem Photobiol A 207:244–253
39. Miyauchi M, Ikezawa A, Tobimatsu H, Irie H, Hashimoto K (2004) Zeta potential and photocatalytic activity of nitrogen doped TiO_2 thin films. Phys Chem 6:865–870
40. Wong M-S, Hsu S-W, Rao KK, Kumar CP (2008) Influence of crystallinity and carbon content on visible light photocatalysis of carbon doped titania thin films. J Mol Catal A 279:20–26
41. Palanivelu K, Im JS, Lee Y-S (2007) Carbon doping of TiO_2 for visible light photocatalysis—A review. Carbon Sci 8:214–224